

RSC Advances



This is an *Accepted Manuscript*, which has been through the Royal Society of Chemistry peer review process and has been accepted for publication.

Accepted Manuscripts are published online shortly after acceptance, before technical editing, formatting and proof reading. Using this free service, authors can make their results available to the community, in citable form, before we publish the edited article. This *Accepted Manuscript* will be replaced by the edited, formatted and paginated article as soon as this is available.

You can find more information about *Accepted Manuscripts* in the [Information for Authors](#).

Please note that technical editing may introduce minor changes to the text and/or graphics, which may alter content. The journal's standard [Terms & Conditions](#) and the [Ethical guidelines](#) still apply. In no event shall the Royal Society of Chemistry be held responsible for any errors or omissions in this *Accepted Manuscript* or any consequences arising from the use of any information it contains.

ARTICLE

Metal-free mesoporous carbon nitride catalyze the Friedel–Crafts reaction by activation of benzene

Cite this: DOI: 10.1039/x0xx00000x

Qiong Yang,^a Wenyao Wang,^a Yanxi Zhao,^a Junjiang Zhu,^{a,*} Yujun Zhu,^b Lihua Wang^{a,*}Received 00th January 2012,
Accepted 00th January 2012

DOI: 10.1039/x0xx00000x

www.rsc.org/

Mesoporous graphitic carbon nitride (mpg-C₃N₄) was synthesized and studied as a metal-free catalyst for Friedel–Crafts acylation of benzene. The synthesis was done by a template method using SiO₂ as template and organic chemicals including guanidine hydrochloride (GndCl), dicyandiamide and urea as precursors. Characterizations by XRD, FT-IR, XPS, N₂ physisorption and TEM indicated that the assumed mpg-C₃N₄ is synthesized irrespective of the precursor used. However, the surface chemistry of mpg-C₃N₄, evaluated from TGA and CO₂-TPD, varied with the precursors and the mass ratio (*r*) of SiO₂ to precursor. Catalytic results showed that the sample prepared using GndCl as precursor and at mass ratio of SiO₂ to GndCl equals to 0.7, defined as mpg-C₃N₄-G_(0.7), exhibits the best activity for the reactions, due to its rich surface basic sites and high surface area. Thus 89% conversion was obtained within 30 min using hexanoyl chloride as electrophile at 90 °C. Even at room temperature (27 °C), 75% conversion can be observed within 30 min. The catalyst is also reusable with ca. 80% activities recoverable after washing with ethanol. The excellent catalytic performances, as well as its low cost, straightforward synthesis and metal-free characters, make mpg-C₃N₄-G_(0.7) a potential catalyst for Friedel–Crafts acylation of benzene in industry with a “green” route.

1. Introduction

Friedel–Crafts (F-C) are one type of useful and important reactions in organic and fine chemistry, and have been applied in industry for the synthesis of chemical intermediates for more than 100 years. Generally, such reactions are catalyzed by stoichiometric excess amount of acid catalysts, e.g., AlCl₃ or FeCl₃,^{1,2} which however produces large amount of waste (ca. 88 wt.%) to the environment and is against the strategy of sustainable development.³ Also, the recycle of the acid catalysts is a challenge for industrial plants. The finding of alternative reagents, which can substitute the current acid catalysts and be recyclable, thus is attractive especially with the more and more strict legislations issued for environmental protection recently.

From the mechanism we know that the role of acid catalysts in the F–C reaction is to activate electrophile participating in the reaction. However, the difficulty of developing sustainable and green acid catalyst for the reaction impels scientists to think if it is possible to catalyze the reaction by activating the nucleophile with a solid base catalyst, in order to avoid the deficiencies of using acid catalysts. Indeed, a recent work by Thomas et al. showed that graphitic carbon nitrides (g-C₃N₄), especially those with mesoporous structure (mpg-C₃N₄), can be promising catalysts for such applications through the activation of nucleophile, other than electrophile, due to their large surface area, rich surface basic sites and the aromatic structure.^{4,5} This is interesting as it is different from the traditional way adopted in industrial plants and even that taught

in the textbook, where the activation of electrophile is suggested. It thus paves a new vista to conduct the Friedel–Crafts reaction with a “green” route.

The material g-C₃N₄ recently receives great interest in many fields, especially in catalysis, because of its easy synthesis and attractive catalytic performances. It can be facilely prepared by polycondensation of a C-, N-, H- and/or O-containing precursor, such as cyanamide,⁶ guanidine hydrochloride (GndCl)⁷ and urea,⁸ in an inert-gas oven at 550°C, and because of its polymer character, mesoporous g-C₃N₄ (mpg-C₃N₄) with varied textural structures and surface chemistries can be synthesized by a template method using SiO₂⁹ or Triton X-100¹⁰ as template for example. In catalysis it has been reported that g-C₃N₄ can be a promising catalyst or catalyst's support for various reactions including photocatalytic split of water or degradation of dyes,^{11–14} NO decomposition,¹⁵ CO₂ activation,^{16,17} Knoevenagel condensations,¹⁸ and selective oxidation or hydrogenation.^{19–22} Because of these promising applications, several review articles^{23–28} on the catalysis use of g-C₃N₄ have been published recently, demonstrating the great interest of g-C₃N₄ in catalysis. It is generally believed that the surface basic sites of g-C₃N₄ are the active sites of reactions, by providing electrons to activate the adsorbed substrates.

Herein we show that mpg-C₃N₄ with varied degrees of condensation, surface chemistries and surface areas can be obtained by a template (SiO₂) method using different precursors or different mass ratios of SiO₂ to precursor, leading to variations in catalytic performances. The mpg-C₃N₄ prepared

using GndCl as precursor and at mass ratio of SiO₂ to GndCl equals to 0.7, mpg-C₃N₄-G_(0.7), exhibits the best activity for Friedel–Crafts acylation of benzene with hexanoyl chloride, with 89% and 75% conversion obtained within 30 min at reaction temperature of 90 and 27 °C, respectively. Further, the catalyst can be well recycled and are active for reactions using various electrophiles. The excellent catalytic performances as well as the wide applicability make mpg-C₃N₄ a promising catalyst for “green” activation of benzene by an F–C route.

2. Experimental

2.1 Synthesis of mpg-C₃N₄

4.0 g precursors (dicyandiamide, GndCl or urea) was first balanced and dissolved in 4 mL deionized water with stirring, and the solution was heated to 50 °C (or 80 °C for dicyandiamide). After the precursors were completely dissolved, a given amount of Ludox (28% dispersion) was added dropwise. The mass ratio (*r*) of SiO₂ to precursor was controlled at 0.4, 0.7 and 1.0, which corresponds to 5.7, 10.0 and 14.3 g Ludox (for dicyandiamide and urea, only *r* = 0.7 was synthesized). After water was evaporated, the resulting white solid was transferred to an air oven and dried at 100 °C overnight, and finally heat-treated in N₂ at 550 °C for 3 h with a heating rate of 3 °C·min⁻¹. Depending on the precursor and the mass ratio of silica to precursor, the sample was named as g-C₃N₄/SiO₂-D_(0.7), g-C₃N₄/SiO₂-U_(0.7) and g-C₃N₄/SiO₂-G_(*r*) (*r* = 0.4, 0.7, 1.0), where “D”, “U” and “G” represent dicyandiamide, urea and GndCl, respectively.

To prepare mesoporous carbon nitride (mpg-C₃N₄), the above obtained composites were treated with 50 mL 4 M NH₄HF₂ for 48 h with drastic stirring to remove the silica template. The powders were then filtrated, washed three times with deionized water and twice with ethanol, and finally dried in a vacuum oven at 50 °C for 6 h. The obtained sample was accordingly named as mpg-C₃N₄-D_(0.7), mpg-C₃N₄-U_(0.7) and mpg-C₃N₄-G_(*r*) (*r* = 0.4, 0.7, 1.0), respectively.

2.2 Characterizations

X-ray diffraction (XRD) patterns were collected using a Bruker D8 Advance X-ray diffractometer with Cu Kα ($\lambda = 1.5406 \text{ \AA}$) irradiation. FT-IR spectra were collected on a Nicolet 470 FTIR spectrometer, working in the range of 400–4000 cm⁻¹ at a resolution of 0.09 cm⁻¹. Thermal gravimetric analysis (TGA) was conducted on a NETZSCH TG 209F3 apparatus. 10 mg samples were first put in an alumina crucible, thereafter air with flow rate of 20 mL min⁻¹ was switched on at room temperature. After reaching a stable baseline, the sample was heated from room temperature to 800 °C at a heating rate of 10 °C min⁻¹, to record the profile. Transmission electron microscopy (TEM) images were obtained on a Tecnai G² 20 S-Twin apparatus with high-resolution transmission electron microscope (200 kV). Before observation the sample was first dispersed in ethanol by ultrasonic method, and then deposited on a copper mesh. N₂ physisorption isotherms were measured on a TriStar II 3020 measurement at liquid nitrogen temperature. Before measurement the sample was treated in vacuum at 150 °C for 5 h. X-ray photoelectron spectroscopy (XPS) spectra were recorded on a VG Multi lab 2000 apparatus using a monochromatic Al Kα X-ray source (300 W) and analyzer pass energy of 25 eV. Binding energies were obtained by referencing to the C (1s) binding energy taken at 284.6 eV.

CO₂-TPD was conducted on a TP-5080 TPD/TPR apparatus (Tianjing Xianquan technology company, China). The sample (80 mg) was first treated in Helium at 150 °C for 1 h and then cooled to room temperature. CO₂ was subsequently switched to the sample for adsorption for 30 min. Thereafter, Helium with flow rate of 30 mL·min⁻¹ was switched again to the sample, and after reaching a stable baseline, the sample was heated from RT to 400 °C at a rate of 10 °C·min⁻¹ to record the profile.

2.3 Catalytic tests

The reaction was carried out in a 50 mL three-necked flask, equipped with a water condenser (temperature was controlled at 5°C). 25 mg catalyst, 0.3 mL benzene, 0.1 mL hexanoyl chloride and 16 mL n-heptane were added to the flask. After the mixture was heated to desired temperature, the reaction was initiated by stirring and the reaction started to count. The reaction mixture was extracted at desired time, centrifuged and analyzed by an Agilent 7890 GC equipped with an FID detector and a HP-5 column. The catalytic activity was evaluated in terms of hexanoyl chloride conversion, as described elsewhere.⁴

3. Results and Discussion

Figure 1A presents the XRD patterns of mpg-C₃N₄ prepared using dicyandiamide, GndCl and urea as precursors. Two characteristic peaks at $2\theta = 12.9^\circ$ and 27.3° , which represent the in-plane structural packing motif and interlayer stacking of aromatic segments, respectively, are observed and can be indexed to the (100) and (002) diffractions of graphitic materials,^{29–31} indicating that the mpg-C₃N₄ is prepared. In comparison, the peak intensity of g-C₃N₄ in the g-C₃N₄/SiO₂ composite is largely attenuated, due to the interference of SiO₂ (see Figure S1A), and the peak of g-C₃N₄/SiO₂-U_(0.7) is even hard to observe, suggesting that the yield or condensation of g-C₃N₄ is different when different precursors are used.

FT-IR spectrum was performed to confirm the formation of g-C₃N₄, Figure 1B. Based on the classification proposed in literature,^{6, 32–35} it is known that the band at 805 cm⁻¹ and that in the range of 1240–1650 cm⁻¹ are attributed to the stretching or bending vibrations of C–N and/or C=N bonds of the triazine rings, the bands at 3100–3500 cm⁻¹ are attributed to the stretching vibrations of N–H bond (=NH or -NH₂ group), and the weak band at near 2175 cm⁻¹ is to the stretching vibration of C≡N group. The presence of N–H bond indicates that the samples are not fully condensed, and there are =NH or -NH₂ groups existing on the edge of g-C₃N₄. These results confirm that the g-C₃N₄ is synthesized. The corresponding IR spectra for g-C₃N₄/SiO₂ composite can be found in Figure S1B, in which the absorption peaks attributed to g-C₃N₄, as well as those to SiO₂ (Si–O–Si bond) and –OH groups are observed.

Figure 1C presents the TGA profiles of the three g-C₃N₄/SiO₂ composites, showing that the loading of g-C₃N₄ prepared with different precursors is different. The loading increases from 12% to 23% and to 45% for samples prepared using urea, GndCl and dicyandiamide as precursor, respectively. This indicates that each precursor undergoes a different polycondensation process and the degree of condensation is different. Urea that contains oxygen atoms in the structure has

the possibility of self-combustion during the polycondensation process, yielding CO_2 and/or H_2O , thus has the least $\text{g-C}_3\text{N}_4$ loading. GndCl that contains volatile HCl in the structure also leads to low $\text{g-C}_3\text{N}_4$ loading as HCl will be released during the polycondensation, without participating in the synthesis process. Dicyandiamide that contains only C, N and H atoms in the structure can be mostly used for the formation of $\text{g-C}_3\text{N}_4$, except the essential release of NH_3 , thus has the highest $\text{g-C}_3\text{N}_4$ loading. This explains why varied $\text{g-C}_3\text{N}_4$ loadings are obtained as different precursors are used, and suggests a different polycondensation process among them.

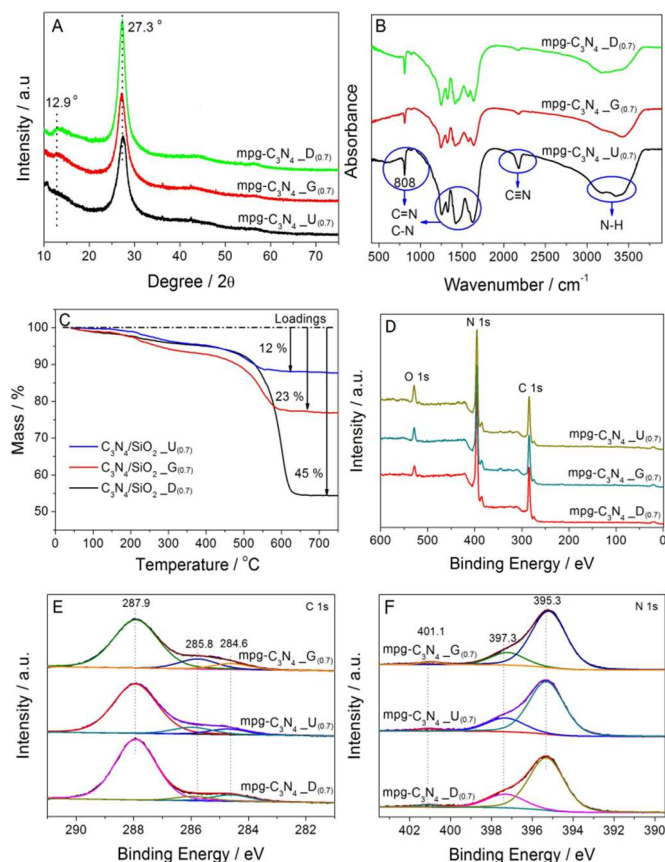


Figure 1. The physicochemical properties of $\text{mpg-C}_3\text{N}_4$ or $\text{g-C}_3\text{N}_4/\text{SiO}_2$ prepared with different precursors and at mass ratio of SiO_2 to precursor equals to 0.7. (A) Wide angle XRD patterns; (B) FT-IR spectrum; (C) TGA curves; (D)-(F) the total and fine XPS spectra for C 1s and N 1s.

Figure 1D-F shows the XPS survey spectrum of the three $\text{mpg-C}_3\text{N}_4$ samples in the range of 0-600 eV, and the corresponding high-resolution spectrum for C 1s and N 1s. The peaks located at binding energy of 283-290, 392-402 and 525-535 eV can be assigned to the C 1s, N 1s and O 1s, respectively, according to the XPS database. The strong peak intensity of C 1s and N 1s indicates that the materials are composed mainly of C and N atoms. By calculation it is found that the surface molar ratio of C/N atoms is slightly different for the three samples but is near 1 (see Table S1), which is higher than the theoretical value (0.75), indicating that there are N defects on the surface of samples. The presence of oxygen atoms could be that the samples were contaminated by oxygen when stored in air, and its surface atomic percentage varied from 3.44 to 7.65% (see Table S1), in sequence of mpg-

$\text{C}_3\text{N}_4\text{-U}_{(0.7)} > \text{mpg-C}_3\text{N}_4\text{-G}_{(0.7)} > \text{mpg-C}_3\text{N}_4\text{-D}_{(0.7)}$. The variation in C/N ratios and the different affinities with oxygen imply that the polycondensation process and surface chemistry of samples prepared using different precursors are not the same, which may lead to variations in their catalytic performances as shown below. No peak assignable to Si 2p (97-105 eV) is observed in the spectrum, confirming that the silica is significantly removed from these mesoporous samples and its influence can be neglected in the reaction. In contrast, strong peak intensity for the O 1s and Si 2p is observed for the supported samples (i.e., $\text{g-C}_3\text{N}_4/\text{SiO}_2$) (see Figure S2).

According to literature, three peaks can be fitted for the C 1s and the N 1s spectrum.³⁶⁻⁴⁰ For C 1s, the binding energy at 284.6, 285.8 and 287.9 eV are assigned to the adventitious carbon, the N-bonded sp^3 hybridized C atoms (C-(N)_3), and the N-bonded sp^2 hybridized C atoms in an aromatic ring (N-C=N), respectively. For N 1s, the main peak at binding energy of 395.3 eV is attributed to the C-N-C groups, the mediate peak at 397.2 eV is to the N-(C)_3 groups, and the weak one at 401.1 eV is to the amino groups carrying hydrogen atoms (C-N-H). It is noted that the peak of tertiary amines is almost 6 times bigger than that of these hydrogen bonded amines, indicating a degree of condensation well beyond the linear polymer melon structure.³⁹

Overall, the above results indicate that $\text{mpg-C}_3\text{N}_4$ can be prepared using SiO_2 as template, but the polycondensation process and surface properties of them vary with the precursors. To provide more information on the textural structure and surface chemistry, three additional characterizations including TEM, N_2 physisorption and CO_2 -TPD were conducted on the selected $\text{mpg-C}_3\text{N}_4\text{-G}$ samples, which showed the best activity in the investigated F-C reactions.

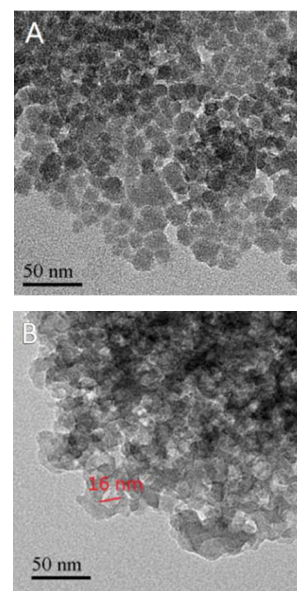


Figure 2. TEM images for the Ludox template and the replicated $\text{mpg-C}_3\text{N}_4\text{-G}_{(0.7)}$

TEM images of the template and the $\text{mpg-C}_3\text{N}_4\text{-G}_{(0.7)}$ are presented in Figure 2, showing that silica in the Ludox solution is homogeneously dispersed with average particle size of ca. 17 nm. As expected, randomly distributed mesoporous pores with pore size of 16 nm are observed for the $\text{mpg-C}_3\text{N}_4\text{-G}_{(0.7)}$, suggesting that the assumed sample is well replicated from the Ludox template.

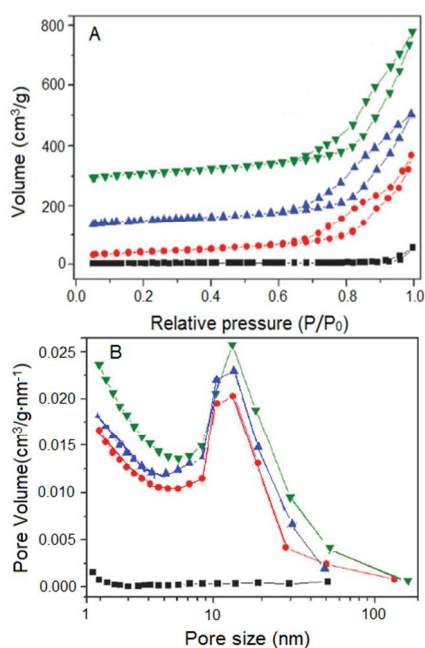


Figure 3. (A) N₂ physisorption isotherms and (B) Pore size distribution of bulk-C₃N₄ (■), mpg-C₃N₄-G_(0.4) (●), mpg-C₃N₄-G_(0.7) (▲) and mpg-C₃N₄-G_(1.0) (▼).

N₂ physisorption isotherms show that a hysteresis loop in the relative pressure of 0.65-1.0, corresponding to a pore size of ca. 14 nm, is observed for mpg-C₃N₄-G_(0.7). Figure 3, indicating the formation of mesoporous structure. The pore size is in well consistent with that obtained from the TEM image (16 nm). The hysteresis loop and pore size are almost the same for mpg-C₃N₄-G_(r) with varied *r* values (*r* = 0.4, 0.7 and 1.0). This is possible as they are prepared using the same template. In contrast, no hysteresis loop and pore is observed for the bulk g-C₃N₄ prepared without template. The corresponding textural data of these samples are listed in Table 1.

Table 1. Textural data of mpg-C₃N₄-G_(r) prepared at different *r* values using GndCl as precursor

Catalyst	BET / m ² g ⁻¹	Pore size / nm	Pore volume/ m ³ g ⁻¹
Bulk-C ₃ N ₄	11	—	0.03
mpg-C ₃ N ₄ -G _(0.4)	144	14.0	0.55
mpg-C ₃ N ₄ -G _(0.7)	166	14.2	0.62
mpg-C ₃ N ₄ -G _(1.0)	151	14.4	0.61

The BET surface area for g-C₃N₄ and mpg-C₃N₄-G_(r) (*r* = 0.4, 0.7 and 1.0) is 11, 144, 166 and 151 m²/g, respectively, with the highest value obtained at *r* = 0.7. The significant increase in the BET surface area from g-C₃N₄ to mpg-C₃N₄-G_(r) suggests that pores are created when template is used. The change in the BET surface area of mpg-C₃N₄-G_(r) is slightly different from that reported by Wang et al.,⁹ who used cyanamide as precursor and found that the surface area increases linearly with the mass ratio of silica to cyanamide. The reason could be that the wall thickness of mpg-C₃N₄ prepared with GndCl as precursor is thinner than that prepared with cyanamide, since the former will release HCl as well as NH₃ during the polycondensation process (see also the TGA profiles above), leading to lower loading or thinner layer of g-

C₃N₄ on the silica support. Thus the pore wall of mpg-C₃N₄-G_(r) would be collapsed during the template leaching process, and this starts to occur at *r* = 1.0 in the present case. Indeed, it is found that the pore volume of mpg-C₃N₄-G_(1.0) is also lower than that of mpg-C₃N₄-G_(0.7), confirming that some pore walls are collapsed.

Figure 4 shows the CO₂-TPD profiles of mpg-C₃N₄-G_(r) (*r* = 0.4, 0.7 and 1.0), with the aim of evaluating the surface basicity of the samples. Two CO₂ desorption peaks locating at 65 and 246 °C are observed for the samples, indicating that there have at least two types of surface basic sites on their surface. The peak area, either for the first or the second, decreases with the increase of *r* (see the data listed in the lower right corner of Figure 4), while no appreciable change in the peak position is observed, indicating that the intensity of surface basicity of the samples is similar. This is possible as they are prepared and treated with the same manner. The decrease in the surface basic sites could be attributed to a more condensed g-C₃N₄ structure, as is observed for CN_x/SBA-15 polycondensed at different temperatures.⁴¹ Therefore, the sample with lower mass loading or prepared at higher mass ratio (*r*) has the chance of forming more condensed structure, as GndCl can be better dispersed at this condition and thus has the possibility of reacting with each other more sufficiently.

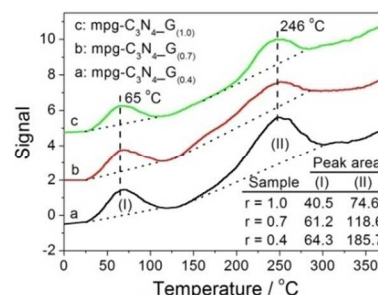


Figure 4. CO₂ TPD profiles of mpg-C₃N₄-G_(r) (*r* = 0.4, 0.7 and 1.0)

The CO₂-TPD profiles of mpg-C₃N₄ prepared with different precursors were also measured and compared in Figure S3, showing that mpg-C₃N₄-G_(0.7) has the biggest peak area for the second CO₂ desorption peak, and the peak area of the first CO₂ desorption peak is slightly smaller than that of mpg-C₃N₄-U_(0.7), while no definite CO₂ desorption peak is observed for mpg-C₃N₄-D_(0.7), indicating that the surface chemistry of sample is significantly different if different precursors are used. Based on the surface structure of g-C₃N₄ proposed in literature³⁴ it is inferred that the first peak is attributed to the desorption of CO₂ adsorbed on the nitrogen site of C-N-C rings, and the second peak is to the amino groups (-NH and/or =NH) on the surface edge. On this basis, it can be inferred that sample mpg-C₃N₄-G_(0.7) has the most amounts of surface amino groups.

Figure 5A presents the catalytic performances of mpg-C₃N₄ prepared with various precursors for F-C acylation of benzene with hexanoyl chloride at reaction temperature of 90 °C, showing that the catalysts are active for the reaction, with 89% conversion obtained from mpg-C₃N₄-G_(0.7) even at 30 min. By comparison, 78% and 57% conversion are obtained from mpg-C₃N₄-D_(0.7) and mpg-C₃N₄-U_(0.7), respectively. This indicates that GndCl is the preferred precursor in the preparation of mpg-C₃N₄ used for F-C reaction. The difference in the activities suggests that there is something different in the mpg-C₃N₄ prepared with different precursors. Considering that they all have the g-C₃N₄ phase structure (see Figure 1), we suspected

that the difference between them must be due to the variations in surface chemistry, such as the amount of surface basic sites.

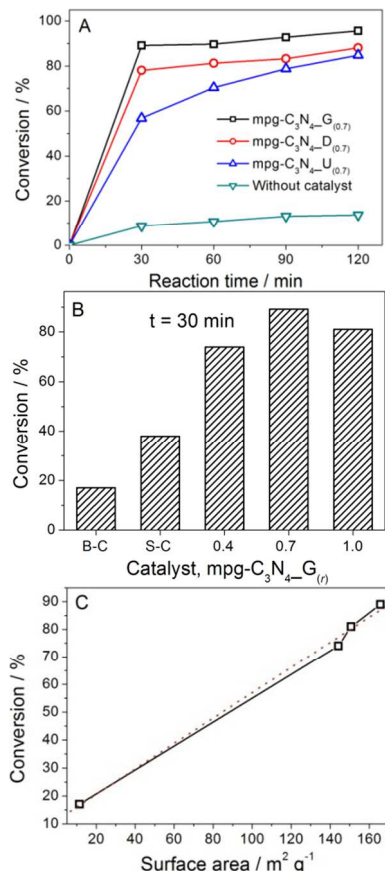


Figure 5. (A) Conversion obtained from mpg-C₃N₄ prepared with various precursors as a function of reaction time; (B) Conversion obtained from bulk g-C₃N₄ (B-C), g-C₃N₄/SiO₂ composites (S-C) and mpg-C₃N₄-G_(r) at reaction time of 30 min; (C) An approximate linearly correlation between the BET surface area of catalysts and the conversions of the reaction. Reaction conditions: 25 mg catalyst, 0.3 mL benzene, 0.1 mL hexanoyl chloride and 16 mL n-heptane, temperature: 90 °C.

Indeed, by correlating the activity with the amount of surface basic site of mpg-C₃N₄-G_(0.7) and mpg-C₃N₄-U_(0.7), it can be found that the second CO₂ desorption peak, corresponding to the amount of amino groups on the surface edge, relates intimately to the activity. In a previous work we have reported that the increase of amino groups (induced by doping Zn in the framework) can improve the activity of g-C₃N₄ for NO decomposition due to an enhanced ability for electron transfer.¹⁵ This supports the above observations as the activation of benzene also requires electrons transferred from the catalyst. Consequently, mpg-C₃N₄-G_(0.7) with the most surface amino groups showed the best activity for F-C reaction. In the following, we thus chose GndCl as precursor to prepare mpg-C₃N₄ for further investigation.

Blank experiment (without catalyst) shows that 15% conversion can be obtained at 120 min, Figure 5A, which is far lower than that conducted in the presence of catalyst (89% for mpg-C₃N₄-G_(0.7) even at 30 min). This indicates that the reaction proceeds mainly by a heterogeneous catalysis, and is catalyzed by the mpg-C₃N₄ catalyst.

A comparison to the supported sample (g-C₃N₄/SiO₂-G_(0.7), abbreviated as “S-C” in Figure 5B), of which the g-C₃N₄

loading is 23 wt.%, shows that the mpg-C₃N₄-G_(0.7) exhibits almost double conversions, Figure 5B, confirming that it is the g-C₃N₄ that catalyzes the reaction. On the other hand, the g-C₃N₄/SiO₂-G_(0.7) shows however higher conversion than the bulk g-C₃N₄ (abbreviated as “B-C” in Figure 5B), although the mass of g-C₃N₄ in the latter is more. This could be that the former has larger surface area (612 m²/g), which is far higher than that of the latter (11.4 m²/g), thus more surface basic sites can be exposed to the substrates, accelerating the reaction rate. That is, surface area is a crucial parameter determining the catalytic performances of g-C₃N₄ for F-C acylation of benzene with hexanoyl chloride.

To study the influence of surface area on the catalytic performances, mpg-C₃N₄-G_(r) with different surface areas but similar pore size (to exclude the influence of pore size) were prepared using the same Ludox template but different mass ratios (*r*) of silica to GndCl. Catalytic tests show that mpg-C₃N₄-G_(0.7) with the largest surface area exhibits the highest activity, and bulk g-C₃N₄ with the smallest surface area exhibits the lowest activity, with an order of mpg-C₃N₄-G_(0.7) > mpg-C₃N₄-G_(1.0) > mpg-C₃N₄-G_(0.4) > Bulk g-C₃N₄, Figure 5B, which fits well to the changes in BET surface area listed in Table 1. Indeed, a correlation between the conversion and the BET surface area shows that the conversion increases almost linearly with the BET surface area, Figure 5C, pointing out the importance of surface area in determining the reaction activity.

It is noted that the changes in activity and surface basic sites counted from CO₂-TPD measurement are not in the same trend for samples prepared with different mass ratio of SiO₂ to GndCl, although the surface basic sites are believed to be the active site of the reaction. Namely, mpg-C₃N₄-G_(0.4) with the most amount of surface basic sites exhibits the lowest activity relative to mpg-C₃N₄-G_(0.7) and mpg-C₃N₄-G_(1.0). The reason could be that the amount of surface basic sites measured by CO₂ cannot be fully applied to the reaction. That is, some surface basic sites (e.g., those in the narrow interspace) that are accessible to CO₂ may not be accessible to benzene, which has larger molecular size (than CO₂), and it seems that only at *r* ≥ 0.7 could the surface basic site be mostly used for benzene adsorption.

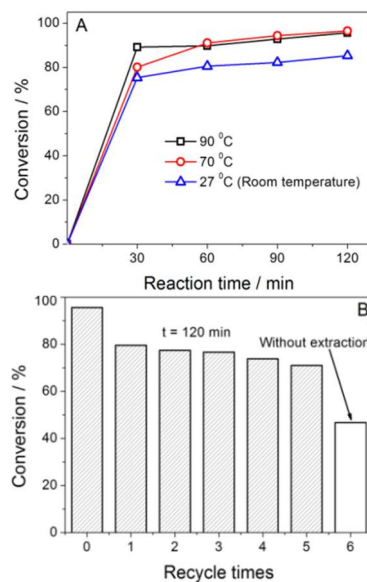


Figure 6. (A) Conversion obtained from mpg-C₃N₄-G_(0.7) at different temperatures; (B) Reusability of mpg-C₃N₄-G_(0.7) in the Friedel–Crafts

acylation of benzene with hexanoyl chloride. Reaction conditions: 25 mg catalyst, 0.3 mL benzene, 0.1 mL hexanoyl chloride and 16 mL n-heptane, temperature: 90 °C.

Because of the high catalytic efficiency of mpg-C₃N₄-G_(0.7) at 90 °C, we have the attempt to see if the catalyst has sufficient capability to catalyze the reaction at a low temperature, with the aim of energy savings. Interestingly, we found that no appreciable loss in the conversion is observed at 70 °C (except that at 30 min), and 75% conversion can be achieved even at room temperature (27 °C), Figure 6A (more can be found in Table S3) indicating that mpg-C₃N₄-G_(0.7) is highly active for the reaction and has the potential of being industrialized. Effects of other reaction conditions including the concentration of substrates, the type of solvents and electrophiles on the reaction are also investigated and the results are listed in Table S2, showing that 1) the catalyst has good ability to catalyze the reaction even at high concentrations, 2) heptane is the optimized solvent for the reaction and 3) the catalyst is active for the Friedel–Crafts acylation of benzene using varied electrophiles.

In the end, the reusability of mpg-C₃N₄-G_(0.7) for the reaction is tested, which is another important parameter in evaluating the possibility of catalyst for industrial use. In each cycle the catalyst was balanced to 25 mg, and the mass of catalyst lost in the filtration process was balanced from a parallel experiment. Figure 6B shows the conversion obtained within 5 cycles. A half decrease in the conversion is observed when the catalyst is reused directly after the reaction (“0” vs. “6”), which could be that 1) the structure of catalyst was destroyed or 2) the active site was blocked (by benzene for example) after the reaction. To check which is the reason accounting for this decrease, we washed the used sample with ethanol several times to extract benzene possibly adsorbed on the catalyst, and then tested its activity again. Results indicate that the activity can be largely recovered after this treatment, thus suggesting that the decreased activity is not attributed to the destruction of catalyst, but to the block of active sites. Indeed, characterizations on the used samples by XRD and FT-IR indicate that the phase structure is not changed and benzene is presented on the surface of the used catalyst, which however can be significantly removed after the ethanol extraction process, see Figure S4. Further optimizations on using a more efficient extraction agent to extract benzene from the surface of catalyst, to release the active site, will be done in our forthcoming work, in order to pave the way of industrialization for the catalyst.

Conclusions

In summary, we showed here that mpg-C₃N₄ can be replicated from a Ludox template with various precursors including dicyandiamide, GndCl and urea. The textural and surface properties of mpg-C₃N₄, such as surface area and surface basic sites, can be controlled by using different precursors or changing the mass ratio (*r*) of template to precursor. Herein, sample prepared using GndCl as precursor and at mass ratio of template to precursor equals to 0.7, mpg-C₃N₄-G_(0.7), shows the best activity to F-C acylation of benzene with hexanoyl chloride, with about 75% conversion even at room temperature (27 °C) within 30 min. Also, the catalyst can be well recycled, especially when a suitable agent is used to extract the benzene adsorbed on its surface. The high reactivity at room temperature and the good reusability of mpg-C₃N₄-G_(0.7) enable it to be a potential catalyst for the F-C reaction in industrial application.

Acknowledgements

Finance support from the National Science Foundation of China (No. 21203253, 21203254), the Natural Science Foundation of Hubei Province of China (2015CFA138), the Science and Technology Activities of Overseas Personnel Preferential Funding Project (No.BZY14038) and the Key Laboratory of Functional Inorganic Material Chemistry, Ministry of Education, Heilongjiang University, is gratefully appreciated.

Notes and references

^a Key Laboratory of Catalysis and Materials Science of the State Ethnic Affairs & Commission Ministry of Education, South-Central University for Nationalities, Wuhan 430074, China

^b Key Laboratory of Functional Inorganic Material Chemistry, Ministry of Education, School of Chemistry and Materials, Heilongjiang University, Harbin, 150080, China

* Corresponding author. E-mail: ciaczjj@gmail.com

Electronic Supplementary Information (ESI) available: Data obtained from XRD, FT-IR, XPS, and CO₂-TPD for the supported g-C₃N₄/SiO₂, mpg-C₃N₄ prepared with different precursors, and the fresh/used mpg-C₃N₄-G_(0.7), and the activity of mpg-C₃N₄-G_(0.7) obtained at different reaction parameters. See DOI: 10.1039/b000000x/

- 1 M. Bandini, A. Melloni, A. Umani-Ronchi, *Angew. Chem. Int. Ed.*, 2004, **43**, 550.
- 2 S.-L. You, Q. Cai, M. Zeng, *Chem. Soc. Rev.*, 2009, **38**, 2190.
- 3 J. H. Clark, *Green Chem.*, 1999, **1**, 1.
- 4 F. Goettmann, A. Fischer, M. Antonietti, A. Thomas, *Angew. Chem. Int. Ed.*, 2006, **45**, 4467.
- 5 F. Goettmann, A. Fischer, M. Antonietti, A. Thomas, *Chem. Commun.*, 2006, **43**, 4530.
- 6 M. Groenewolt, M. Antonietti, *Adv. Mater.*, 2005, **17**, 1789.
- 7 J. Xu, H.T. Wu, X. Wang, B. Xue, Y.X. Li, Y. Cao, *Phys. Chem. Chem. Phys.*, 2013, **15**, 4510.
- 8 F. Dong, L. Wu, Y. Sun, M. Fu, Z. Wu, S.C. Lee, *J. Mater. Chem.*, 2011, **21**, 15171.
- 9 X.C. Wang, K. Maeda, X.F. Chen, K. Takanebe, K. Domen, Y.D. Hou, X.Z. Fu, M. Antonietti, *J. Am. Chem. Soc.*, 2009, **131**, 1680.
- 10 Y. Wang, X. Wang, M. Antonietti, Y. Zhang, *ChemSuschem*, 2010, **3**, 435.
- 11 Y. Zheng, L. Lin, X. Ye, F. Guo, X. Wang, *Angew. Chem. Int. Ed.*, 2014, **53**, 11926.
- 12 M. Zhang, X. Wang, *Energ. Environ. Sci.*, 2014, **7**, 1902.
- 13 K. Kailasam, J.D. Epping, A. Thomas, S. Losse, H. Junge, *Energ. Environ. Sci.*, 2011, **4**, 4668.
- 14 H. Xu, J. Yan, Y. Xu, Y. Song, H. Li, J. Xia, C. Huang, H. Wan, *Appl. Catal. B: Environ.*, 2013, **129**, 182.
- 15 J.J. Zhu, Y.C. Wei, W.K. Chen, Z. Zhao, A. Thomas, *Chem. Commun.*, 2010, **46**, 6965.
- 16 F. Goettmann, A. Thomas, M. Antonietti, *Angew. Chem. Int. Ed.*, 2007, **46**, 2717.
- 17 H. Shi, G. Chen, C. Zhang, Z. Zou, *ACS Catal.*, 2014, **4**, 3637.
- 18 F. Su, M. Antonietti, X. Wang, *Catal. Sci. Technol.*, 2012, **2**, 1005.
- 19 P. Zhang, Y. Gong, H. Li, Z. Chen, Y. Wang, *RSC Adv.*, 2013, **3**, 5121.

Journal Name

- 20 Y. Wang, J. Yao, H. Li, D. Su, M. Antonietti, *J. Am. Chem. Soc.*, 2011, **133**, 2362.
- 21 J.J. Zhu, S.A.C. Carabineiro, D. Shan, J.L. Faria, Y.J. Zhu, J.L. Figueiredo, *J. Catal.*, 2010, **274**, 207.
- 22 T. Yuan, H. Gong, K. Kailasam, Y. Zhao, A. Thomas, J. Zhu, *J. Catal.*, 2015, **326**, 38.
- 23 Y. Wang, X. Wang, M. Antonietti, *Angew. Chem. Int. Ed.*, 2012, **51**, 68.
- 24 Y. Zheng, J. Liu, J. Liang, M. Jaroniec, S.Z. Qiao, *Energ. Environ. Sci.*, 2012, **5**, 6717.
- 25 X. Wang, S. Blechert, M. Antonietti, *ACS Catal.*, 2012, **2**, 1596.
- 26 X.-H. Li, M. Antonietti, *Chem. Soc. Rev.*, 2013, **42**, 6593.
- 27 J. Zhu, P. Xiao, H. Li, S.A.C. Carabineiro, *ACS Appl. Mater. Interfaces*, 2014, **6**, 16449.
- 28 Y. Gong, M. Li, H. Li, Y. Wang, *Green Chem.*, 2015, **17**, 715.
- 29 S.C. Yan, Z.S. Li, Z.G. Zou, *Langmuir*, 2010, **26**, 3894.
- 30 Z. Jin, N. Murakami, T. Tsubota, T. Ohno, *Appl. Catal. B: Environ.*, 2014, **150–151**, 479.
- 31 Y. Xu, W.D. Zhang, *Eur. J. Inorg. Chem.*, 2015, **2015**, 1744.
- 32 S. Hwang, S. Lee, J.-S. Yu, *Appl. Surf. Sci.*, 2007, **253**, 5656.
- 33 E.G. Gillan, *Chem. Mater.*, 2000, **12**, 3906.
- 34 V.N. Khabashesku, J.L. Zimmerman, J.L. Margrave, *Chem. Mater.*, 2000, **12**, 3264.
- 35 Q. Guo, Y. Xie, X. Wang, S. Zhang, T. Hou, S. Lv, *Chem. Commun.*, 2004, **1**, 26.
- 36 L. Ge, C. Han, *Appl. Catal. B: Environ.*, 2012, **117–118**, 268.
- 37 Q. Xiang, J. Yu, M. Jaroniec, *J. Phys. Chem. C*, 2011, **115**, 7355.
- 38 Y. Yang, Y. Guo, F. Liu, X. Yuan, Y. Guo, S. Zhang, W. Guo, M. Huo, *Appl. Catal. B: Environ.*, 2013, **142–143**, 828.
- 39 A. Thomas, A. Fischer, F. Goettmann, M. Antonietti, J.O. Muller, R. Schlogl, J.M. Carlsson, *J. Mater. Chem.*, 2008, **18**, 4893.
- 40 Y. He, Y. Wang, L. Zhang, B. Teng, M. Fan, *Appl. Catal. B: Environ.*, 2015, **168–169**, 1.
- 41 P. Xiao, Y.X. Zhao, T. Wang, Y.Y. Zhan, H.H. Wang, J.L. Li, A. Thomas, J.J. Zhu, *Chem. Eur. J.*, 2014, **20**, 2872.